Specific Recognition of CG Base Pairs by 2-Deoxynebularine within the Purine·Purine·Pyrimidine Triple-Helix Motif†

Hans Ulrich Stilz and Peter B. Dervan*

Beckman Institute, California Institute of Technology, Pasadena, California 91125

Received September 18, 1992; Revised Manuscript Received December 11, 1992

ABSTRACT: The sequence-specific recognition of double-helical DNA by oligodeoxyribonucleotide-directed triple-helix formation is limited mostly to purine tracts. Within the geometric constraints of the phosphate–deoxyribose position of a purine·purine·pyrimidine triple-helical structure, model building studies suggested that the deoxyribonucleoside 2′-deoxynebularine (dN) might form one specific hydrogen bond with cytosine (C) or adenine (A) of Watson–Crick cytosine–guanine (CG) or adenine–thymine (AT) base pairs. 2-Deoxynebularine (dN) was incorporated by automated methods into purine-rich oligodeoxyribonucleotides. From affinity cleavage analysis, the stabilities of base triplets within a purine·purine·pyrimidine (Pu·Pu·Py) triple helix were found to decrease in the order N·CG ~ N·AT ≫ N·GC ~ N·TA (pH 7.4, 37 °C). Oligodeoxyribonucleotides containing two N residues were shown to bind specifically within plasmid DNA a single 15 base pair site of the human immunodeficiency virus genome containing two CG base pairs within a purine tract. This binding event occurs under physiologically relevant pH and temperature (pH 7.4, 37 °C) and demonstrates the utility of the new base. Quantitative affinity cleavage titration reveals that, in the particular sequence studied, an N·CG base triplet interaction results in a stabilization of the local triple-helical structure by 1 kcal·mol^{-1} (10 mM NaCl, 1 mM spermine tetrahydrochloride, 50 mM Tris–acetate, pH 7.4, 4 °C) compared to an A·CG base triplet mismatch.

Oligodeoxyribonucleotide-directed triple-helix formation provides one of the most versatile methods for the sequence-specific recognition of double-helical DNA (Moser & Dervan, 1987; Le Doan et al., 1987; Cooney et al., 1988; Beal & Dervan, 1991). The ability to target a broad range of DNA sequences, the high stabilities of the triple-helical complexes, and the apparent sensitivity to single-base mismatches make this a powerful technique for binding single sites within large segments of double-helical DNA (Singleton & Dervan, 1992a). This structural motif has been utilized to mediate single-site-specific cleavage of human chromosomal DNA (Strobel et al., 1991), to inhibit DNA binding proteins (Maher et al., 1989; Hanvey et al., 1990; Francois et al., 1989), and to inhibit gene expression in vitro (Cooney et al., 1988; Maher et al., 1992).

At least two classes of DNA triple helices exist which differ in the sequence composition of the third strand, the relative orientations and positions of the backbones of the three strands, and the base triplet interactions. Pyrimidine-rich oligodeoxyribonucleotides bind specifically to extended purine tracts of double-helical DNA in the major groove parallel to the Watson–Crick (WC) purine strand through the formation of specific Hoogsteen hydrogen bonds to the purine WC bases (Moser & Dervan, 1987; Le Doan et al., 1987; Rajogopal & Feigon, 1989; Radhakrishnan et al., 1991a). Specificity is derived from thymime (T) recognition of adenine–thymine base pairs (T·AT base triplets) and protonated cytosine (C^+) recognition of guanine–cytosine base pairs (C^+·GC base triplets). The number of double-helical sequences capable of being recognized by this motif has been extended by the base triplet G·TA (Griffin & Dervan, 1989; Kiessling et al., 1992), by the incorporation of nonnatural bases into the oligodeoxyribonucleotides (Ono et al., 1991a; Koh & Dervan, 1992; Kiessling et al., 1992; Krawczyk et al., 1992; Griffin et al., 1992), and by the design of 3′–3′ and 5′–5′ linked pyrimidine oligodeoxyribonucleotides for alternate-strand triple-helix formation (Horne & Dervan, 1990; Ono et al., 1991b).

Within the second triple-helix motif purine-rich oligodeoxyribonucleotides bind in the major groove of DNA antiparallel to the purine Watson–Crick strand through the formation of specific hydrogen bonds (Cooney et al., 1988; Beal & Dervan, 1991; Pilch et al., 1991; Durland et al., 1991; Radhakrishnan et al., 1991b). Sequence specificity is imparted by G recognition of guanine–cytosine base pairs (G·GC base triplets) and adenine (A) as well as thymine (T) recognition of adenine–thymine base pairs (A·AT and T·AT base triplets).

Recently, the two families of triple-helical structures (Pu·Pu·Py and Pu·Pu·Py) have been employed to create intramolecular alternate strand triple helices (Jayasena & Johnston, 1992) and to recognize double-helical sequences containing all four base pairs by alternate-strand triple-helix formation with oligodeoxyribonucleotides containing only natural 3′–5′ phosphodiester linkages (Beal & Dervan, 1992a).

Unfortunately, the sequence-specific recognition of double-helical DNA by purine oligodeoxyribonucleotide-directed triple-helix formation is limited mostly to purine tracts (Beal & Dervan, 1992b). Design leads that could expand the recognition code to pyrimidine–purine base pairs (CG, TA) would provide one step toward a general solution for targeting single sites in megabase size DNA. We describe here our initial efforts to design a heterocycle for the recognition of CG Watson–Crick base pairs within the Pu·Pu·Py triple-helix structural motif. Model-building studies suggested that the deoxyribonucleoside 2′-deoxynebularine (dN)[1] could fulfill this role (Figure 1). Our model assumes that the purine of

† We are grateful to the Office of Naval Research for generous support.
* To whom correspondence should be addressed.

0006-2960/93/0432-2177$04.00/0

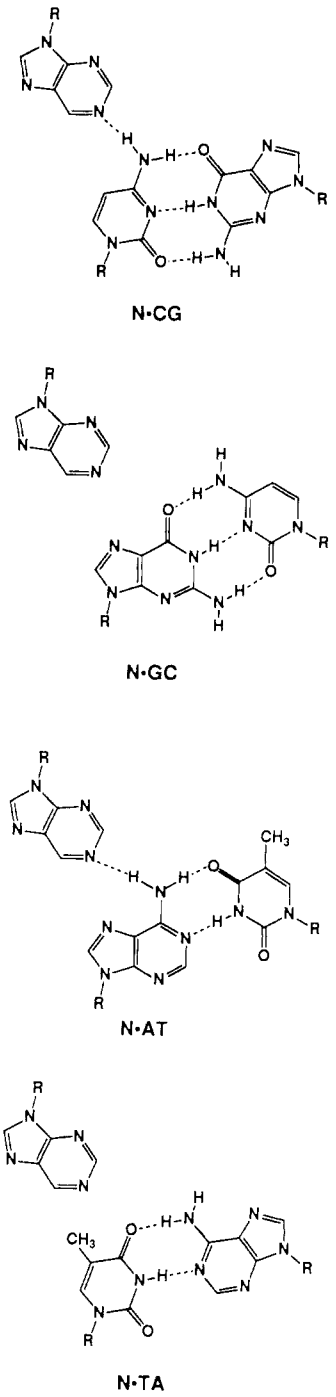

FIGURE 1: Models representing base triplets N·AT, N·CG, N·GC, and N·TA formed between 2′-deoxynebularine and the Watson–Crick duplex within the Pu·Pu·Py triple helix. All bases are depicted with anti glycosidic bonds (Radhakrishnan et al., 1991b), and the phosphate–deoxyribose backbone of the third strand is antiparallel to the Watson–Crick purine strand.

nebularine (N) (i) is in the anti glycosidic conformation, (ii) would allow favorable base stacking interactions in the third strand, and (iii) provides a hydrogen bond acceptor (N1) to the exocyclic amino group of cytosine or adenine (Figure 1).

EXPERIMENTAL PROCEDURES

Materials and General Methods. The deoxynebularine phosphoramidite was purchased from Glen Research. All other phosphoramidites and chemicals for DNA synthesis were obtained from Applied Biosystems Inc. Restriction endonucleases and all other enzymes were purchased from Boehringer-Mannheim, New England Biolabs, or Sigma. Restriction endonucleases were used according to the supplier's recommended protocol in the activity buffer provided. The Sequenase DNA sequencing kit (Version 2.0) was obtained from United States Biochemical Inc. Deoxynucleoside triphosphates (100 mM solutions), calf thymus DNA, and Nick columns were purchased from Pharmacia LKB. Glycogen was obtained from Boehringer-Mannheim as a 20 mg/mL aqueous solution. The radiolabeled triphosphates 5′-(α-^{32}P)-dGTP (>3000 Ci/mmol), 5′-(γ-^{32}P)ATP (>5000 Ci/mmol), and 5′-(α-^{35}S)dATP (>1000 Ci/mmol) were obtained from Amersham. All other chemicals were of analytical or HPLC grade. Whenever possible, standard molecular biological methods were used (Sambrook et al., 1989).

Synthesis of Oligodeoxyribonucleotides. Oligodeoxyribonucleotides were synthesized on an Applied Biosystems Model 380B DNA synthesizer using standard solid-phase β-cyanoethyl phosphoramidite triester chemistry (Beaucage & Caruthers, 1981; Sinha et al., 1984). The thymidine–EDTA nucleoside analog (T*) was prepared according to published procedures and was incorporated at the 3′ end of oligodeoxyribonucleotides via the 5′-*O*-DMT–thymidine–EDTA–triethyl ester–3′-succinyl controlled pore glass (Dreyer & Dervan, 1985). Unmodified oligodeoxyribonucleotides were deprotected in concentrated ammonium hydroxide at 55 °C for 24 h. Oligodeoxyribonucleotides containing the nucleoside analog T* were treated with 0.1 N NaOH (1.5 mL) at 55 °C for 24 h. The 5′-*O*-DMT-protected oligomers were purified by reverse-phase FPLC chromatography (Pharmacia ProRPC 15-μm HR 10/10; gradient of 0–40% acetonitrile in 100 mM triethylammonium acetate, pH 7.0). Lyophilized fractions were treated (20 min, 24 °C) with an 80% solution of acetic acid in water (500 μL) in order to remove the DMT protecting group. The oligomers were then repurified by FPLC. The concentrations of the oligodeoxyribonucleotides were determined by UV measurements (A_{260}), using the following molar extinction coefficients: 15 400 (A), 11 700 (G), 7300 (C), 8800 (T and T*), and 6000 (N) cm^{-1} M^{-1}. Oligodeoxyribonucleotide solutions were divided into samples containing 1 and 5 nmol each and lyophilized to dryness for storage at −78 °C.

HPLC Analysis. Analytical HPLC was performed with a Hewlett-Packard 1090 liquid chromatograph using a reverse-phase VYDAC 201HS54 4.6-mm × 25-cm 5-μm C18 column. The purified oligodeoxyribonucleotides (3 nmol) were digested simultaneously with snake venom phosphodiesterase (3 μL, 2.4 μg/μL) and calf intestine alkaline phosphatase (3 μL, 1 unit/μL) in 50 mM Tris-HCl (pH 8.1) and 100 mM $MgCl_2$. The reaction mixture was incubated at 37 °C for 3 h, filtered through a 0.45-μm Nylon-66 syringe filter (Rainin), and lyophilized. The sample was dissolved with 10 μL of 10 mM ammonium phosphate (pH 5.1)/8% methanol buffer, and an aliquot of the solution was injected onto the C18 reverse-phase column. The products were eluted with 10 mM ammonium phosphate (pH 5.1)/8% methanol and detected at A_{260}. Comparison with standard solutions of dA, dG, dT,

[1] Abbreviations: bp, base pair(s); DMT, 4,4′-dimethoxytrityl; dN, 2-deoxynebularine; EDTA, ethylenediaminetetraacetic acid; FPLC, fast protein liquid chromatography; HIV, human immunodeficiency virus; HPLC, high-performance liquid chromatography; IPTG, isopropyl β-D-thiogalactoside; N, nebularine; nt, nucleotides; SD, standard deviation; T*, thymidine modified at C-5 with EDTA (Dreyer & Dervan, 1985); TAE, Tris–acetate/EDTA; TBE, Tris–borate/EDTA; Tris, tris(hydroxymethyl)aminomethane; X-Gal, 5-bromo-4-chloro-3-indolyl β-D-galactoside; Z·XY, a nucleotide base triplet where Z defines the nucleotide in the third strand.

and dN established the composition of the oligodeoxyribonucleotides.

Preparation of 5'-Labeled 39-mer Duplex. For the preparation of the duplex targets, each single-stranded oligodeoxyribonucleotide (100 pM) of sequence composition 5'-AATTCTCTCTAAAAAGGGXGGGGAGGGGAGGGA-AAAACTCTCT-3' (X = A, G, C, or T) was 5' end labeled using T4 polynucleotide kinase and (γ-^{32}P)ATP. The reaction mixture was extracted three times with TE-saturated phenol and three times with chloroform/isoamyl alcohol (24:1). The DNA was precipitated, and the radiolabeled oligodeoxyribonucleotides were annealed to their unlabeled complementary oligodeoxyribonucleotides. The resulting duplexes were purified on 15% nondenaturing polyacrylamide gels (19:1 monomer/bis). Gel bands were visualized by autoradiography, and desired bands were excised from the gel, crushed, and eluted with 1 mL of a 200 mM NaCl solution at 37 °C for 20 h. The eluents were passed through 0.45-μm Centrex filters and lyophilized. The residue was taken up in 100 μL of distilled water, and the solution was then desalted on a Nick column. The radiolabeled duplex–DNA was finally isolated by precipitation, washed twice with 70% ethanol, and dissolved in water to a final concentration of 10 000 cpm/μL.

Affinity Cleaving Reactions of 39-mer Duplex Targets. Specific DNA cleavage reactions of adenine were performed as described previously (Iverson & Dervan, 1987). The affinity cleaving reactions were executed in a total volume of 80 μL by combining a mixture of oligodeoxyribonucleotide–EDTA (100 nM) and $Fe(NH_4)_2(SO_4)_2{\cdot}6H_2O$ (250 nM) with the 5'-^{32}P-labeled duplex (~120 000 cpm) in a solution of Tris–acetate (50 mM, pH 7.4 at 24 °C), NaCl (20 mM), spermine tetrahydrochloride at pH 7.4 (100 μM), and calf thymus DNA (100 μM in base pairs). The oligodeoxyribonucleotide was allowed to equilibrate with the DNA duplex target at 37 °C for 4 h. The cleavage reactions were then initiated by the addition of dithiothreitol (4 mM final concentration) and allowed to proceed at 37 °C for 14 h. The reactions were quenched by freezing followed by lyophilization. The residue was suspended in 10 μL of formamide–TBE loading buffer (90% formamide, 10% 10 × TBE buffer, 0.02% bromophenol blue, 0.2% xylene cyanol) and transferred to new tubes. The DNA suspensions were assayed for specific activity by scintillation counting and diluted to 5000 cpm/μL with more formamide–TBE loading buffer. The cleavage products were denatured at 90 °C for 5 min, and 4 μL of each sample was separated by 20% denaturing polyacrylamide gel electrophoresis (19:1, monomer/bis). The gels were exposed to X-ray film (Amersham Hyperfilm-MP) at −78 °C with a single intensification screen or to a storage phosphor screen.

Construction of the Plasmid pULHIV. The plasmid pULHIV was obtained by cloning the oligonucleotides 5'-AATTCGGCAAGAGGCGAGGGGCGGCGACT-3' and 5'-CTAGAGTCGCCGCCCCTCGCCTCTTGCCG-3' into the large *Eco*RI/*Xba*I restriction fragment of pUC19 using T4 DNA ligase. The ligation mixture was employed to transform Epicurian Coli XL1 Blue competent cells (Stratagene). Plasmid isolation was performed using QIAGEN purification kits (Diagen) according to the manufacturer's protocol, and the sequence of the insert was subsequently confirmed by dideoxynucleotide sequencing (Sanger et al., 1977) using the M13 reverse sequencing primer (New England Biolabs, 1201).

Preparation of 3'-^{32}P-Labeled EcoO109I–SspI Restriction Fragment of pULHIV. Plasmid DNA (20 μg) was linearized with *Eco*O109I, precipitated, and the end-labeled with 5'-(α-^{32}P)dGTP employing Sequenase (Version 2.0). Unincorporated radiolabeled nucleotide triphosphates were removed by filtration of the reaction mixture through a Nick column. The labeled DNA was precipitated and digested with *Ssp*I. The resulting 3'-^{32}P-end labeled fragment (2515 bp) was purified by agarose gel electrophoresis (2% Nusieve GTG agarose, FMC). Gel bands were visualized by autoradiography, and the desired band was excised from the gel. The agarose was disrupted using three freeze–thaw cycles. Following centrifugation of the resulting suspension, the supernatant was removed and washed three times with TE-saturated phenol and three times with chloroform/isoamyl alcohol (24:1). The DNA was precipitated, dissolved in 100 μL of TE, and desalted on a Nick column. Finally, the DNA was precipitated, washed twice with 70% ethanol, and dissolved in water to a final concentration of 10 000 cpm/μL.

Affinity Cleaving Reactions of the pULHIV EcoO109I–SspI Restriction Fragment. The affinity cleaving reactions were executed in a total volume of 80 μL by combining a mixture of oligodeoxyribonucleotide–EDTA (2 μM) and $Fe(NH_4)_2(SO_4)_2{\cdot}6H_2O$ (5 μM) with the 3'-^{32}P-labeled restriction fragment (~40 000 cpm) in a solution of Tris–acetate (50 mM, pH 7.4 at 24 °C), NaCl (10 mM), spermine tetrahydrochloride at pH 7.4 (1 mM), and calf thymus DNA (100 μM in base pairs). The oligodeoxyribonucleotide was allowed to equilibrate with the DNA duplex target at 37 °C for 4 h. The cleavage reactions were then initiated by the addition of dithiothreitol (4 mM) and allowed to proceed at 37 °C for 12 h. The reactions were stopped by precipitation of the DNA. The residue was resuspended in TE and transferred to new tubes. The DNA solutions were assayed for specific activity by scintillation counting and diluted to 250 cpm/μL. Glycerol gel loading buffer (30% glycerol in water, 0.25% bromophenol blue, 0.25% xylene cyanol) was added to each of the samples, and the cleavage products were separated by 5% nondenaturing polyacrylamide gel electrophoresis (19:1, monomer/bis). The gel was dried on a slab dryer and visualized by autoradiography (Amersham Hyperfilm-MP, −78 °C, intensification screen).

Preparation of 3'-^{32}P-Labeled HindIII–SspI Restriction Fragment of pULHIV. Following linearization of the plasmid (20 μg) with *Hin*dIII the DNA was end-labeled, isolated as above, and digested with *Ssp*I. The digestion products were separated on a 5% nondenaturing polyacrylamide gel (19:1, monomer/bis). The gel band corresponding to the labeled 638-bp fragment was excised. The gel pieces were crushed and soaked in 1 mL of a solution containing 10 mM Tris-HCl (pH 8.0) and 25 mM EDTA (pH 8.0) at 37 °C for 20 h. The eluent was passed through a 0.45-μm Centrex filter, washed three times each with TE-saturated phenol and chloroform/isoamyl alcohol (24:1), and lyophilized. The residue was dissolved in 100 μL of TE, and the DNA was desalted on a Nick column, precipitated, washed twice with 70% ethanol, and resuspended in distilled water at a final activity of 20 000 cpm/μL. The total radioactivity of the isolated restriction fragment was usually 1×10^6–3×10^6 cpm, corresponding to a lower limit for the specific activity of the radiolabeled DNA fragment of 1×10^8–3×10^8 cpm/nmol of 638-bp DNA fragment.

Quantitative Affinity Cleavage Titrations. In a typical quantitative affinity cleaving experiment, involving 18 data lanes and 1 control lane per gel, a stock solution containing labeled target DNA in association buffer was prepared by mixing 80 μL of 0.5 M Tris–acetate buffer at pH 7.4, 40 μL of 200 mM NaCl, 80 μL of calf thymus DNA (1.0 mM bp),

10 μL of 3′-end-labeled target DNA, and 30 μL of distilled water. The stock solution was then distributed among 19 1.5-mL microcentrifuge tubes in 12-μL aliquots. A dried pellet of the oligodeoxyribonucleotide–EDTA (5 nmol) was dissolved in a solution of aqueous $Fe(NH_4)_2(SO_4)_2 \cdot 6H_2O$ to produce a solution that was 100 μM in oligodeoxyribonucleotide and 250 μM in Fe(II). The oligodeoxyribonucleotide–EDTA·Fe(II) solution was allowed to equilibrate for 15 min at 24 °C and was then diluted serially by the addition of 10 μL of the respective oligodeoxyribonucleotide–EDTA·Fe(II) solution to 90 μL of distilled water, resulting in oligodeoxyribonucleotide–EDTA·Fe(II) solutions of the following concentrations: 100 μM (undiluted), 10 μM, 1 μM, 100 nM, 10 nM, and 1 nM. To each reaction tube were added 4 μL of oligodeoxyribonucleotide–EDTA·Fe(II) at the appropriate concentration, 4 μL of 10 mM spermine tetrahydrochloride at pH 7.4, and distilled water to a final volume of 36 μL. The oligodeoxyribonucleotide–EDTA·Fe(II) and the DNA were allowed to equilibrate for 48 h at 4 °C. The cleavage reactions were initiated by the addition of 4 μL of a 40 mM DTT solution to each tube. The reactions were incubated for 12 h at 4 °C. The cleavage reactions were quenched by the addition of EDTA, glycogen, NaOAc (pH 5.2), and $MgCl_2$ to final concentrations of 1.0 mM, 70 μg/mL, 280 mM, and 10 mM, respectively. The DNA was precipitated, washed with 70% ethanol, and dissolved in 20 μL of distilled water. The solutions were frozen, and the solvent was removed by lyophilization. The DNA in each tube was resuspended in 5 μL of formamide–TBE loading buffer, and the solutions were transferred to new tubes, assayed for specific activity by scintillation counting, and diluted to 1000 cpm/μL with more formamide–TBE loading buffer. The DNA was denatured at 90 °C for 5 min, and 5 μL of each sample was loaded onto an 8% denaturing polyacrylamide gel (19:1, monomer/bis). The gel was dried on a slab dryer and then exposed to a storage phosphor screen at 24 °C.

Storage Phosphor Technology Autoradiography. Photostimulable storage phosphor imaging plates (Kodak screen S0230 obtained from Molecular Dynamics; Johnston et al., 1990) were pressed flat against gel samples and exposed in the dark at 24 °C for 4 h (20% gels) or 12–24 h (dried 8% gels). ImageQuant software (Molecular Dynamics v. 3.0) and a Molecular Dynamics 400S PhosphorImager were used to obtain and analyze data from the storage screens.

Quantitation of Cleavage Efficiencies. The radiation background of the screen was determined by performing volume integrations over four separate sites, which were not exposed to the gel surface. All other volume integrations were based on the averaged background value obtained. Integration of the cleavage bands was performed over the five most efficiently cleaved nucleotides. Rectangles of the same size were used for each lane, and the amount of radioactivity found in the appropriate control lanes containing untreated DNA was subtracted from the obtained values. The cleavage efficiencies were evaluated by calculating the ratio of the radioactivity of the site-specific cleavage band by the integrated volume of the entire lane. The given values represent the average over two independent experiments.

Affinity Cleavage Titration Data Analysis. The data were analyzed as described previously (Singleton & Dervan, 1992a,b). Briefly, the cleavage intensities found in the site (I_{tot}) and reference blocks (I_{ref}) were determined by performing volume integrations of the target site and reference blocks, respectively, and the site-specific cleavage (I_{site}) for all oligodeoxyribonucleotide concentrations was calculated:

$$I_{site} = I_{tot} - \lambda I_{ref} \quad (1)$$

The constant λ was calculated using the average of the ratios of I_{tot} to I_{ref} from each of the three lowest oligodeoxyribonucleotide concentrations. A theoretical binding curve was fit to the experimental data using the apparent maximum cleavage ($I_{sat.}$) and the K_T as the adjustable parameters:

$$I_{fit} = I_{sat.} \frac{K_T[O]_{tot}}{1 + K_T[O]_{tot}} \quad (2)$$

The difference between I_{fit} and I_{site} for all data points was minimized using the nonlinear least-squares fitting procedure of Kaleidagraph software (Version 2.1; Abelbeck Software). The fits were performed without weighting the data points. All data points were included unless visual inspection of the computer image from a storage phosphor screen revealed a flaw at either the target site or reference blocks, or the I_{site} value for a single lane was greater than two standard deviations (SD) away from the respective values of the neighboring lanes. Data from experiments for which fewer than 75% of the data lanes were usable were discarded. SD among different experimental measurements of K_T were 30–100% of the mean K_T. Each reported K_T value is the mean of three to five experimental determinations ± 1 SD.

RESULTS

Synthesis and Base Composition Analysis of Oligodeoxyribonucleotides Containing 2′-Deoxynebularine. A series of 15mer oligodeoxyribonucleotides **1–17** containing one or two 2′-deoxynebularine nucleoside residues (dN) were synthesized by standard solid-phase methods. The 2′-deoxynebularine phosphoramidite coupled as efficiently as the dA, dG, dC, and dT phosphoramidites. The base compositions of oligodeoxyribonucleotides **1**, **6**, **11**, **16**, and **17** containing 2′-deoxynebularine were established by enzymatic degradation and subsequent HPLC analysis. The oligodeoxyribonucleotides were treated with snake venom phosphodiesterase and calf intestine phosphatase. The nucleoside monomers obtained were separated by HPLC and identified by their HPLC retention times and UV spectra. Comparison of the integrated areas of the HPLC peaks with that of standard solutions of dA, dG, dT, and dN confirmed the correct base composition of the oligodeoxynucleotides.

Analysis of Binding Specificity. The relative affinity of nebularine (N) for all four Watson–Crick base pairs within a Pu·Pu·Py triple helix was examined by affinity cleaving (Dreyer & Dervan, 1985). A series of five 15mer oligodeoxyribonucleotides **1–5** (Figure 2A), differing at one base position, 5′-TGGGGTGGGGZGGGT*-3′ (**Z** = N, A, G, C, or T), and equipped with the DNA cleaving moiety, thymidine–EDTA·Fe(II) (T*), at the 3′ end were prepared. The relative stabilities of the triple-helical structures formed upon complexation of these five oligodeoxyribonucleotides with four 39-bp DNA duplexes containing one variable base pair site 5′-^{32}P-AATTCTCTCTAAAAAGGGXGGGGAGGGGA-GGGAAAAACTCT-CT-3′·5′-CTAGAGAGAGTTTTTC-CCTCCCCTCCCCYCCCTTTTTAGAGAG-3′ (**XY** = AT, CG, GC, or TA) were then measured. The DNA affinity cleaving reactions were performed under conditions which allowed single mismatch base triplets to be distinguished (100 nM oligodeoxyribonucleotide–EDTA, 100 μM spermine tetrahydrochloride, 20 mM NaCl, pH 7.4, 37 °C) (Beal & Dervan, 1992b). Of the 20 triplets examined the most efficient cleavage and hence most stable triplets were found for the

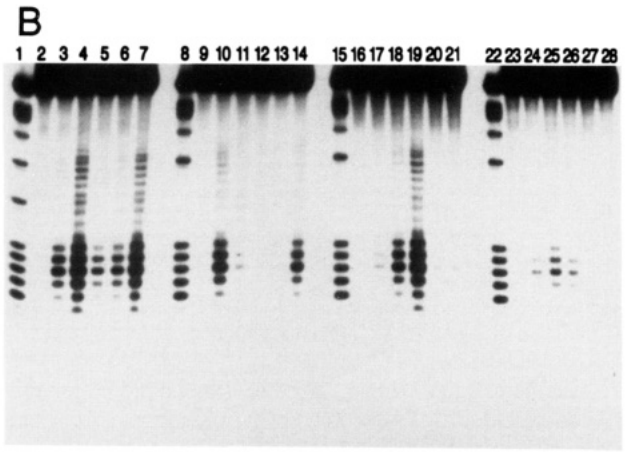

FIGURE 2: (A) The sequences of oligodeoxynucleotide–EDTA **1–5** are shown, where T* indicates the position of thymidine–EDTA (Dreyer & Dervan, 1985). The oligodeoxyribonucleotides differ at one base position indicated in bold type to the four common natural DNA bases (A, G, C, T) and to nebularine (N). Also represented are the sequences of the target oligodeoxyribonucleotide duplexes. The box indicates the double-stranded sequence bound by oligodeoxyribonucleotides–EDTA·Fe(II) **1–5**. The Watson–Crick base pair (AT, GC, CG, or TA) opposite the variant base in the oligodeoxyribonucleotide is in bold type. The heights of the arrows represent the relative cleavage efficiencies at the indicated bases as determined by quantitative analysis using storage phosphor autoradiography. Only the major nucleotide positions of cleavage are shown for simplicity. (B) Autoradiogram of a 20% denaturing polyacrylamide gel. (Lanes 1, 8, 15, and 22) Products of an adenine–specific cleaving reaction (Iverson & Dervan, 1987) on 5′-end-labeled 5′-^{32}P-AATTCTCTCTAAAAAGGG**X**GGGGAGGGGAGGGAAAAAC-TCTCT-3′·5′-CTAGAGAGAGTTTTTCCCTCCCCTCCCC**Y**-CCCTTTTTAGAGAG-3′. **XY** = AT (lane 1), **XY** = CG (lane 8), **XY** = GC (lane 15), **XY** = TA (lane 22). (Lanes 2, 9, 16, and 23) Control showing intact 5′-labeled 39-bp DNA standard obtained after treatment according to the cleavage reactions in the absence of oligodeoxynucleotide–EDTA. **XY** = AT (lane 2), **XY** – CG (lane 9), **XY** = GC (lane 16), **XY** = TA (lane 23). (Lanes 3–7, 10–14, 17–21, 24–28) DNA cleavage products produced by oligodeoxyribonucleotides–EDTA·Fe(II) **1–5**. **1** (lanes 3, 10, 17, and 24), **2** (lanes 4, 11, 18, and 25), **3** (lanes 5, 12, 19, and 26), **4** (lanes 6, 13, 20, and 27), **5** (lanes 7, 14, 21, and 28). **XY** = AT (lanes 3–7), **XY** = CG (lanes 10–14), **XY** = GC (lanes 17–21), **XY** = TA (lanes 24–28).

combinations **Z** = A or T, **XY** = AT, and **Z** = G, **XY** = GC (Figure 2B, lanes 4, 7, and 19). This result reflects the known ability of G, A, and T to form stable G·GC, A·AT, and T·AT base triplets, respectively (Beal & Dervan, 1991). Importantly, strong binding and cleavage was also detected for a N·CG triplet (Figure 2B, lane 10). The base triplets N·AT, C·AT, T·CG, and A·GC (Figure 2B, lanes 3, 6, 14, and 18) produced moderate cleavage. Weak cleavage was observed for the 12 additional triplet combinations. The cleavage efficiencies were measured using storage phosphor analysis (Johnston et al., 1990) (Figure 3). For the triple helices containing deoxynebularine, the relative order of stabilities was N·CG ~ N·AT ≫ N·GC ~ N·TA (pH 7.4, 37 °C).

Site-Specific Double-Strand Cleavage of Plasmid DNA. In order to determine whether 2′-deoxynebularine can be used to target a purine-rich tract containing a few CG base pairs within a larger segment of double-helical DNA, a plasmid containing the purine-rich target sequence 5′-AGAGGC-

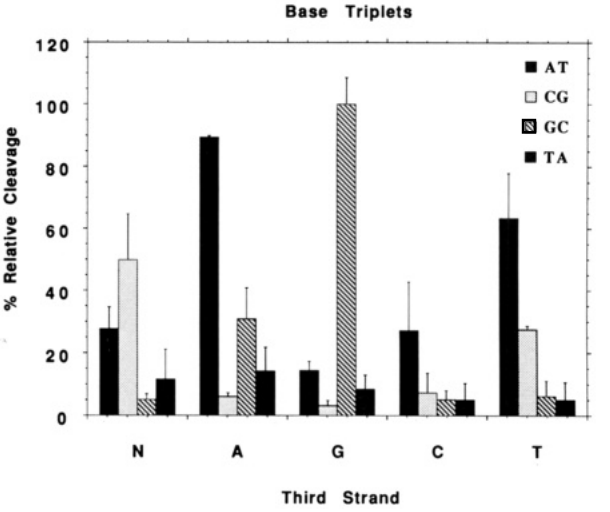

FIGURE 3: Histogram depicting relative cleavage efficiencies (normalized) for the 20 base triplets. The values were obtained by PhosphorImager quantitative analysis and represent the mean ± SD of two determinations.

GAGGGGCGG-3′·5′-CCGCCCCTCGCCTCT-3′, which occurs naturally in the HIV genome (Ratner et al., 1985), was cloned into pUC19 (pUlHIV). The ability of oligodeoxyribonucleotides **6–17** (Figure 4A) to bind specifically to the target sequence was examined by affinity cleaving under conditions sensitive for a single mismatch (2 μM oligodeoxyribonucleotide–EDTA, 1 μM spermine tetrahydrochloride, 10 mM NaCl, pH 7.4, 37 °C). A 2.51-kbp *Eco*O109I–*Ssp*I restriction fragment of pULHIV, which contains the target sequence located 0.42 kbp from the 3′-^{32}P-labeled end, was isolated (Figure 4A). This restriction fragment was allowed to react with oligodeoxynucleotides–EDTA·Fe(II) **6–17** of sequence composition 5′-GG**Z2**GGGG**Z1**G**Z2**GG**Z1**GT*-3′, which differ at four variable positions (**Z1** = A, T, or N; **Z2** – N, A, G, C, or T), in the presence of dithiothreitol at 37 °C (pH 7.4). The cleavage products were separated by 5% nondenaturing polyacrylamide gel electrophoresis. One major cleavage site, 0.42 kbp in size, indicating sequence-specific cleavage was observed only for the oligonucleotides **6** (**Z1** = A; **Z2** = N), **10** (**Z1** = A; **Z2** = T), **11** (**Z1** = T; **Z2** = N), and **15** (**Z1** = T; **Z2** = T), respectively (Figure 4B, lanes 3, 7, 8, and 12).

Energetics of an N·CG Base Triplet by Quantitative Affinity Cleavage Titration. In order to measure the energetics for the N·CG base triplet interaction, the equilibrium association constant for the binding of an oligodeoxyribonucleotide–EDTA·Fe(II) (O) to a single DNA site (D) on a plasmid fragment was measured using quantitative affinity cleavage titration (Singleton & Dervan, 1992a,b):

$$O + D \overset{K_T}{\rightleftharpoons} T \overset{k_{cl}}{\rightarrow} P_{cl} \qquad (3)$$

The rationale behind the method is that the amount of product fragments (P_{cl}) produced during an affinity cleavage experiment is proportional to the fractional occupancy (θ) of the duplex target site by the oligodeoxyribonucleotide–EDTA·Fe, where K_T represents the equilibrium association constant and k_{cl} the pseudo-first-order rate constant for the formation of the cleavage products from the complex, T.

Because K_T can be expressed as a function of θ and the equilibrium concentration of unbound O ($[O]_{eq}$), an equation relating signal intensity produced by the products of sequence-

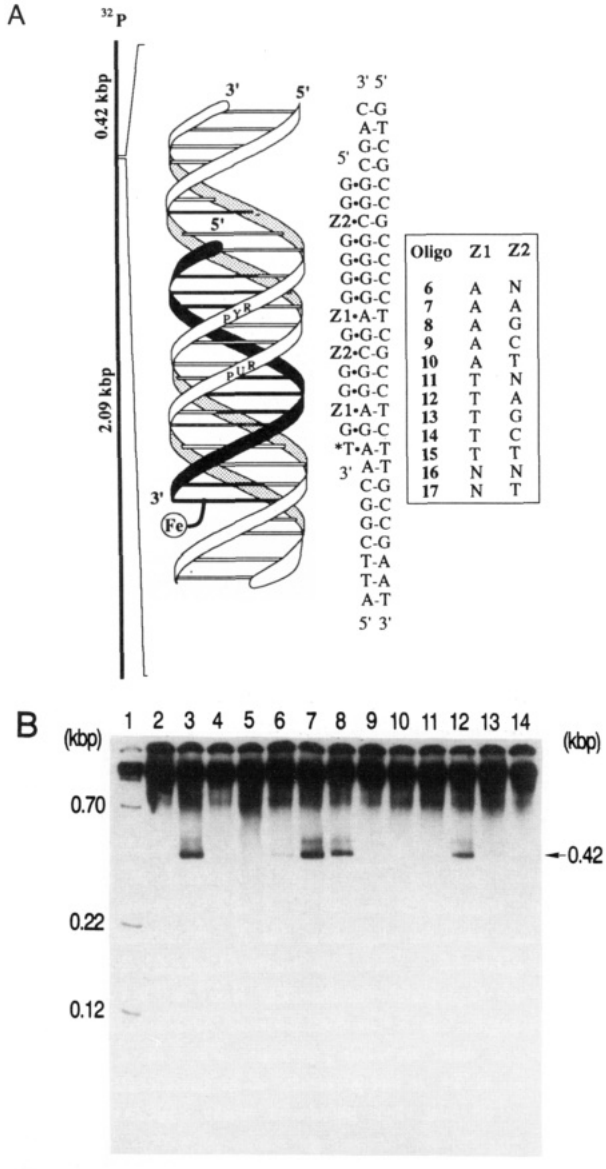

FIGURE 4: (A) Ribbon model and sequence of the triple-helix complex between a single site in the pULHIV *Eco*O109I–*Ssp*I restriction fragment and oligodeoxyribonucleotides–EDTA **6–17**. The purine oligodeoxyribonucleotide with EDTA·Fe(II) at the 3′ termini is located near the center of the major groove of the double-helical DNA antiparallel to the purine strand (Beal & Dervan, 1991). The target site is located 0.42 kbp from the ^{32}P-radiolabeled end of the restriction fragment. (B) Double-strand cleavage of pULHIV *Eco*O109I–*Ssp*I restriction fragment analyzed on a 5% nondenaturing polyacrylamide gel. (Lane 1) Molecular size markers obtained by ^{32}P labeling of λ-DNA *Bst*EII digest. Sizes of the λ fragments are indicated on the left side of the autoradiogram. (Lane 2) Control showing intact 3′-labeled pULHIV *Eco*O109I–*Ssp*I restriction fragment (2515 bp) standard obtained after treatment according to the cleavage reactions in the absence of oligodeoxyribonucleotide–EDTA. (Lanes 3–14) DNA cleavage products produced by oligodeoxyribonucleotides–EDTA·Fe(II) **6–17**, respectively. The expected size of the cleavage product is given on the right side of the autoradiogram.

specific cleavage (I_{site}) to K_T can be derived:

$$I_{site} = I_{sat.}\frac{K_T[O]_{tot}}{1 + K_T[O]_{tot}} \quad (4)$$

where I_{sat} is the signal intensity produced at saturation binding ($\theta = 1$). Importantly, the use of radiolabeled DNA allows the total concentration of DNA to be less than 5% of the total concentration of O ($[O]_{tot}$) and thus allows us to use the approximation $[O]_{tot} = [O]_{eq}$. Therefore, by measuring the

FIGURE 5: The sequence (shaded box) and relative position of the 15-bp triple helix target site within the pULHIV *Hin*dIII–*Ssp*I restriction fragment are shown at the top. The sequences of the oligodeoxyribonucleotides **6**, **7**, **10**, **11**, and **17**, where **T*** indicates the position of thymidine–EDTA, are depicted at the bottom.

site-specific affinity cleavage produced by bound oligodeoxyribonucleotide–EDTA·Fe(II) as a function of $[O]_{tot}$, an empirical titration binding isotherm can be constructed and K_T can be determined from nonlinear least-squares analysis of the ($[O]_{tot}$, I_{site}) data points.

Using this method the association constants for oligodeoxyribonucleotides–EDTA·Fe(II) **6**, **7**, **10**, **11**, and **17** binding to a 638-bp DNA duplex were measured. For this, 5′-^{32}P-end-labeled duplex DNA and various concentrations of an oligodeoxyribonucleotide–EDTA·Fe(II) (100 pM–50 mM) were mixed in association buffer (10 mM NaCl, 1 mM spermine tetrahydrochloride, 50 mM Tris–acetate, 0.1 mM bp calf thymus DNA, pH 7.4) and incubated at 4 °C. The association reactions were allowed to equilibrate for 48 h, and the cleavage reactions were subsequently initiated by addition of DTT. The cleavage reactions were allowed to proceed for 12 h at 4 °C. The maximum site-specific cleavage yield observed under these conditions was about 15%. The cleavage products were separated by polyacrylamide gel electrophoresis under strand-denaturing conditions. The results of a representative experiment performed employing oligodeoxyribonucleotide–EDTA·Fe **11** are shown in Figure 6. The amounts of radiolabeled DNA in the bands at the target cleavage site and at a reference site were measured from a photostimulable storage phosphor autoradiogram (Figure 6). The I_{site} data points were calculated according to eq 1, and the ($[O]_{tot}$, I_{site}) data points were fitted using a nonlinear least-squares method, with K_T and $I_{sat.}$ as adjustable parameters (eq 2). The mean values of the association constants for **6**, **7**, **10**, **11**, and **17** were each extracted from three to five such experiments (Table I). The data points obtained were averaged and are plotted along with average best-fit titration binding isotherms (Figure 7).

DISCUSSION

9-β-D-Ribofuranosylpurine (nebularine) is a naturally occurring nucleoside found in certain mushrooms and active against Mycobacteria (Löfgren & Luning, 1953; Löfgren et al., 1954). The syntheses of nebularine and deoxynebularine have been described (Fox et al., 1958; Nair & Chamberlain, 1984). Model-building studies suggested that nebularine (N) could be employed to recognize CG base pairs within the Pu·Pu·Py triple-helical structural motif. 2′-Deoxynebularine (dN) can be incorporated into oligodeoxyribonucleotides without complications (Eritja et al., 1986). For the oligode-

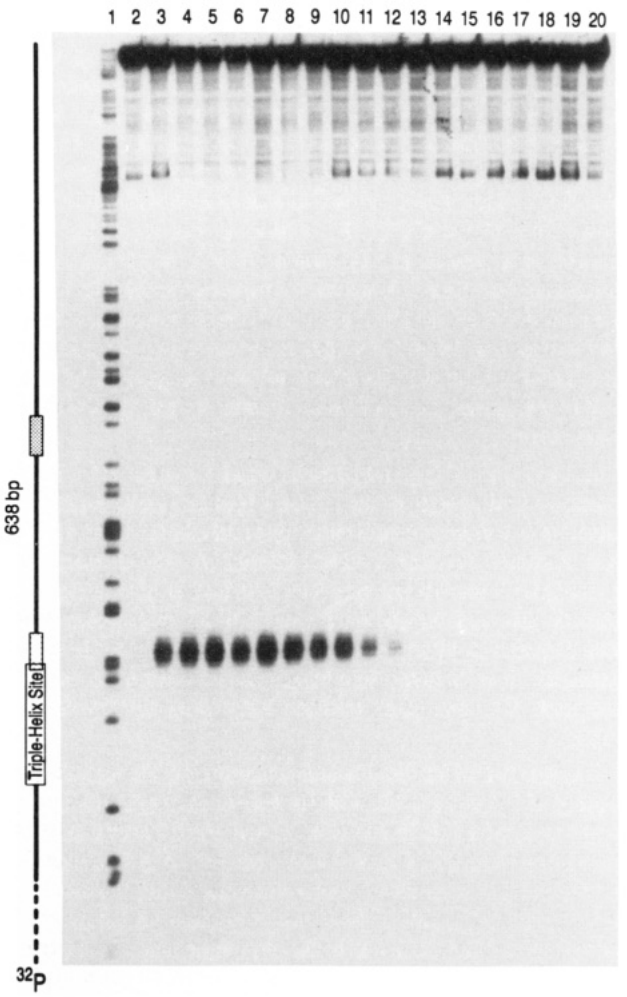

FIGURE 6: Autoradiogram of an 8% denaturing polyacrylamide gel used to separate the cleavage products generated by **11**·Fe(II) from a quantitative affinity cleavage experiment performed in association buffer (10 mM NaCl, 1 mM spermine tetrahydrochloride at pH 7.4, 50 mM Tris–acetate, pH 7.4) at 4 °C. The bar drawn on the left of the autoradiogram indicates the position of the 15-bp duplex target site (white box), the bands used to measure I_{tot} (shaded box), and the bands used to measured to I_{ref} (hatched box). (Lane 1) Products of an adenine-specific cleavage reaction. (Lane 2) Intact 3′-labeled duplex obtained after incubation in association buffer at 4 °C in the absence of oligodeoxyribonucleotide–EDTA·Fe(II) and DTT. (Lanes 3–20) DNA affinity cleavage products produced by **11**·Fe(II) at various concentrations: 50 μM (lane 3); 20 μM (lane 4); 10 μM (lane 5), 5 μM (lane 6); 2 μM (lane 7); 1 μM (lane 8); 500 nM (lane 9); 200 nM (lane 10); 100 nM (lane 11); 50 nM (lane 12); 20 nM (lane 13); 10 nM (lane 14); 5 nM (lane 15); 2 nM (lane 16); 1 nM (lane 17); 500 pM (lane 18); 200 pM (lane 19); 100 pM (lane 20).

Table I: Association Constants at pH = 7.4 and 4 °C[a]

oligo	base triplets (n)[b]	K_T (M^{-1})	ΔG_T (kcal·mol^{-1})
6	G·GC (10), A·AT (2), N·CG (2)	$5.0 (\pm 1.8) \times 10^7$	−9.8 (±0.3)
7	G·GC (10), A·AT (2), A·CG (2)	$1.3 (\pm 0.5) \times 10^6$	−7.8 (±0.3)
10	G·GC (10), A·AT (2), T·CG (2)	$1.2 (\pm 0.3) \times 10^8$	−10.2 (±0.3)
11	G·GC (10), T·AT (2), N·CG (2)	$8.6 (\pm 2.0) \times 10^7$	−10.1 (±0.2)
17	G·GC (10), N·AT (2), T·CG (2)	$2.7 (\pm 2.0) \times 10^6$	−8.2 (±0.8)

[a] Values listed are mean values measured from affinity cleavage titration experiments performed in association buffer (10 mM NaCl, 1 mM spermine tetrahydrochloride, 0.1 mM bp calf thymus DNA, 50 mM Tris–acetate, pH 7.4). [b] n = number of triplets within each triple-helical complex.

oxyribonucleotides described here this was confirmed by enzymatic degradation and subsequent HPLC analysis. Affinity cleavage studies demonstrate that nebularine (N) binds to CG base pairs. The binding affinity observed for the

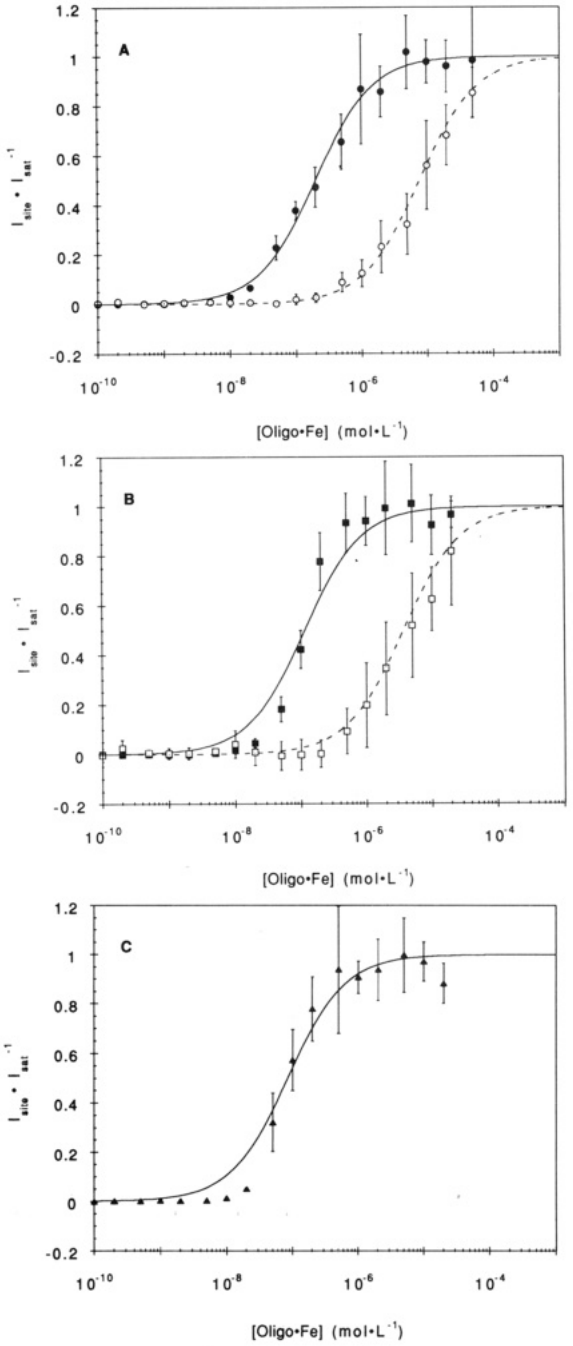

FIGURE 7: (A) Data from quantitative affinity cleavage experiments involving oligodeoxyribonucleotides **6**·Fe(II) (●) and **7**·Fe(II) (○) in association buffer at 4 °C. The data points represent the average site-specific cleavage signal intensities ± SD from three [**6**·Fe(II)] and four [**7**·Fe(II)] independent experiments. The sigmoidal curves show the titration binding isotherms plotted using the mean values of K_T for **6**·Fe(II) and **7**·Fe(II) (Table I) and eq 4. The data points were normalized using $I_{sat.}$ from each experiment, and the binding curves were subsequently normalized using $I_{sat.} = 1$ for eq 4. (B) Data from quantitative affinity cleavage experiments involving oligodeoxyribonucleotides **11**·Fe(II) (■) and **17**·Fe(II) (□) in association buffer at 4 °C. The data points represent the average site-specific cleavage signal intensities ± SD from four [**11**·Fe(II)] and five [**7**·Fe(II)] independent experiments. The sigmoidal curves show the titration binding isotherms plotted using the mean values of K_T for **11**·Fe(II) and **17**·Fe(II) (Table I) and eq 4. The data points and fit binding curves were normalized as above. (C) Data from quantitative affinity cleavage experiments involving oligodeoxyribonucleotide **10**·Fe(II) (▲) in association buffer at 4 °C. The data points represent the average site-specific cleavage signal intensities ± SD from three independent experiments. The sigmoidal curve shows the titration binding isotherm plotted using the mean value of K_T for **10**·Fe(II) (Table I) and eq 4. The data points and the fit binding curve were normalized as above.

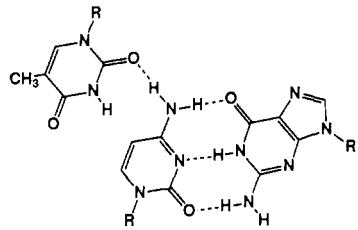

T·CG

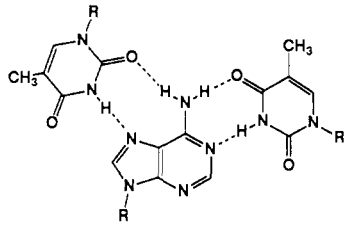

T·AT

FIGURE 8: Models representing base triplets T·CG and T·AT formed between thymidine and the CG or AT Watson–Crick base pairs within the purine·purine·pyrimidine triple helix. All bases are depicted with anti glycosidic bonds (Radhakrishnan et al., 1991b), and the phosphate–deoxyribose backbone of the third strand is antiparallel to the Watson–Crick purine strand.

N·CG base triplet, however, is smaller than those found for the conventional base triplets G·GC, A·AT, and T·AT (Figure 3). The formation of the G·GC, A·AT, and T·AT base triplets is probably mediated by two specific hydrogen bonds as well as favorable stacking interactions (Beal & Dervan, 1991, 1992b). In contrast, model studies suggest that 2′-deoxynebularine would form only one specific hydrogen bond to CG base pairs, which is consistent with the lower binding affinity observed (Figure 1). Moderate cleavage is observed for the N·AT base triplet as well, implying that N may also form a specific hydrogen bond to AT base pair. On the other hand, the low cleavage efficiency observed for the base triplets N·GC and N·TA indicates that no stabilizing interactions exist between 2′-deoxynebularine and GC or TA base pairs (Figure 2B; lanes 17 and 24).

The cleavage efficiency found for a N·AT triplet is less than that found for a N·CG triplet (Figure 2B; lanes 3 and 10). The two-dimensional molecular models do not suggest an explanation for the observed preferential binding of 2′-deoxynebularine to CG base pairs. Undoubtedly, there will be sequence composition effects on the stabilities of triple-helical complexes (Kiessling et al., 1992). It is conceivable that the particular sequence studied here leads to stacking interactions and a tertiary structure which permits a more favorable hydrogen bonding interaction with the exocyclic amino group of cytosine.

As is apparent from the data in Figure 2B, thymidine is the only natural base which binds to some extent to CG base pairs. The formation of the T·CG base triplet is probably mediated by the formation of one specific hydrogen bond (Figure 8; Beal & Dervan, 1992b). However, since thymidine, in contrast to nebularine, interacts preferentially with the AT base pair, it cannot be considered as a solution to specific recognition of CG (Figures 2B and 8). The stabilizing interactions for the C·AT and A·GC triplets have been rationalized by the formation of a single hydrogen bond between the third strand base and duplex base pair (Beal & Dervan, 1992b).

The above results indicate that 2′-deoxynebularine-containing oligodeoxyribonucleotides recognize CG base pairs within short duplex DNA. In order to ascertain whether the stabilizing interaction of the N·CG triplet can be applied to the recognition of CG base pairs within other sequences and in the context of site-specific targeting within larger DNA, further experiments were carried out using a 2510-bp restriction fragment. The purine-rich sequence containing two CG base pairs, 5′-AGAGGCGAGGGGCGG-3′·5′-CCGCCCCTCGCCTCT-3′, which is found in the HIV genome, was chosen as representative of a target site having biological relevance. A set of 12 oligonucleotides **6**–**17** was selected, first, to test the ability of 2′-deoxynebularine versus the four natural bases to recognize two internal CG base pairs and, second, to study the effect on this recognition of using A·AT as opposed to T·AT base triplets within the Pu·Pu·Py triple helix.

As anticipated, oligonucleotides **6** and **11** cause site-specific double-strand breaks in the 2.5-kb fragment under conditions sensitive to a single mismatch (Figure 4B, lanes 3 and 8). The data demonstrate that 2′-deoxynebularine can be employed to recognize a purine site with two cytosines at physiologically relevant pH and temperature (pH 7.4, 37 °C). Also, since both oligodeoxyribonucleotides bind specifically to the target sequence, it is evident that either A or T may be used to recognize AT base pairs without disturbing the N·CG base triplet.

Comparison of the association constants for the equilibrium binding of **6** and **11** to the 638-bp restriction fragment duplex target in association buffer at 4 °C and pH 7.4 confirms these qualitative findings (Figure 7 and Table I). The free energies of binding for oligodeoxyribonucleotides **6** and **11** are −9.8 (±0.3) and −10.1 (±0.2) kcal·mol^{-1}, respectively, and are in agreement within the error of the determination. In contrast, the association constant for binding of **7**, which contains two single, internal A·CG base triplet mismatches, is clearly reduced from those of **6** and **11** (Figure 7A,B and Table I). The differences in binding free energy between **6** and **7** indicate that replacing two A·CG base triplet interactions with two N·CG base triplet interactions results in a 2 kcal·mol^{-1} increase of stability of the triple-helical complex over two mismatched A·CG triplets. These changes in the free energy of binding are consistent with an average free energy difference $\Delta\Delta G$ of 1 kcal·mol^{-1} between an A·CG base triplet and a N·CG base triplet at 4 °C and pH 7.4, although we expect these average free energy differences to be affected by nearest neighbor interactions. This average free energy difference is smaller than those found for a single internal base triplet mismatch (2.5–3.0 kcal·mol^{-1}) within the Py·Pu·Py motif of triple-helix formation at 24 °C and pH 7.0 (Singleton & Dervan, 1992a). This further indicates that the N·CG base triplet is less stable than the conventional base triplets G·GC, A·AT, and T·AT.

The specific binding of oligodeoxyribonucleotides **10** and **15** to the duplex target reveals that a T·CG base triplet interaction would also allow recognition of CG base pairs (Figure 4B, lanes 8 and 12). The free energy of binding for oligodeoxyribonucleotide **10**, ΔG_T of −10.2 (±0.3) kcal·mol^{-1}, is similar to the value found for oligodeoxyribonucleotide **6**. These data indicate that N·CG and T·CG base triplets are of comparable strength. However, since oligodeoxyribonucleotides **16** and **17** do not bind to the target sequence, this indicates that N·AT base triplets are weaker than T·AT base triplets (Figure 4B, lanes 13 and 14). Comparison of the K_T values for the equilibrium binding of **11**, K_T = 8.6 (±2.0) × 10^7 M^{-1}, and **17**, K_T = 2.7 (±2.0) × 10^6 M^{-1}, to the duplex target in association buffer at 4 °C and pH 7.4 strongly supports this result (Figure 7B and Table I). The differences

in binding free energy between **11** and **17** of 1.9 kcal·mol^{-1} emphasize that 2′-deoxynebularine allows a more specific recognition of CG base pairs than thymidine within a Pu·Pu·Py triple helix.

CONCLUSION

The use of the 2′-deoxynebularine (dN) within a purine oligodeoxyribonucleotide extends triple-helix specificity to three of the four possible base pairs of the double-helical DNA. However, the N·CG base triplet interaction is not as stabilizing as the G·GC, A·AT, or T·AT base triplets. It is therefore not obvious how far one can deviate from homopurine–homopyrimidine target sequences and still obtain triple-helix formation. Undoubtedly, the relative stabilities of N·CG and N·AT base triplets are likely to depend on sequence composition. However, this result provides a useful structural lead for the construction of modified nebularine heterocycles which may provide a higher affinity and increased specificity for CG base pairs by oligonucleotide-directed recognition of double-helical DNA within the Pu·Pu·Py triple-helix motif.

ACKNOWLEDGMENT

We are grateful to the Deutsche Forschungsgemeinschaft for a postdoctoral fellowship to H.U.S.

REFERENCES

Beal, P. A. & Dervan, P. B. *Science 251*, 1360–1363.
Beal, P. A., & Dervan, P. B. (1992a) *J. Am. Chem. Soc. 114*, 4976–4982.
Beal, P. A., & Dervan, P. B. (1992b) *Nucleic Acids Res. 20*, 2773–2776.
Beaucage, S. L., & Caruthers, M. H. (1981) *Tetrahedron Lett. 22*, 1859–1862.
Cooney, M., Czernuszewicz, G., Postel, E. H., Flint, S. J., & Hogan, M. E. (1988) *Science 241*, 456–459.
Dreyer, G. B., & Dervan, P. B. (1985) *Proc. Natl. Acad. Sci. U.S.A. 82*, 968–972.
Durland, R. H., Kesseler, D. J., Gunnell, S., Duvic, M., Pettitt, B. M., & Hogan, M. E. (1991) *Biochemistry 30*, 9246–9255.
Eritja, R., Horowitz, D. M., Walker, P. A., Ziehler-Martin, J. P., Boosalis, M. S., Goodman, M. F., Itakura, K., & Kaplan, B. E. (1986) *Nucleic Acids Res. 14*, 8135–8153.
Fox, J. J., Wempen, I., Hampton, A., & Doerr, I. L. (1958) *J. Am. Chem. Soc. 80*, 1669–1675.
Francois, J.-C., Saison-Behmoaras, T., Thuong, N. T., & Helene, C.(1989) *Biochemistry 28*, 9617–9619.
Griffin, L. C., & Dervan, P. B. (1989) *Science 245*, 967–971.
Griffin, L. C., Kiessling, L. L., Beal, P. A., Gillespie, P., & Dervan, P. B. (1992) *J. Am. Chem. Soc. 114*, 7976–7982.
Hanvey, J. C., Shimizu, M., & Wells, R. D. (1990) *Nucleic Acids Res. 18*, 157–161.
Horne, D. A., & Dervan, P. B. (1990) *J. Am. Chem. Soc. 112*, 2435–2437.
Iverson, B. L., & Dervan, P. B. (1987) *Nucleic Acids Res. 15*, 7823–7830.
Jayasena, S. D., & Johnston, B. H. (1992) *Biochemistry 31*, 320–327.
Johnston, R. F., Pickett, S. C., & Barker, D. L. (1990) *Electrophoresis 11*, 355–360.
Kiessling, L. L., Griffin, L. C., & Dervan, P. B. (1992) *Biochemistry 31*, 2829–2834.
Koh, J. S., & Dervan, P. B. (1992) *J. Am. Chem. Soc. 114*, 1470–1478.
Krawczyk, S. H., Milligan, J. F., Wadwani, S., Moulds, C., Froehler, B. C., & Matteucci, M. D. (1992) *Proc. Natl. Acad. Sci. U.S.A. 89*, 3761–3764.
Le Doan, T., Perrouault, L., Praseuth, D., Habhoub, N., Decout, J.-L., Thuong, N. T., Lhomme, J., & Helene, C. (1987) *Nucleic Acids Res. 15*, 7749–7760.
Löfgren, N., & Luning, R. (1953) *Acta Chem. Scand. 7*, 225.
Löfgren, N., Luning, R., & Hedstrom, H. (1954) *Acta Chem. Scand. 8*, 670–680.
Maher, L. J., III, Wold, B., & Dervan, P. B. (1989) *Science 245*, 725–730.
Maher, L. J., III, Dervan, P. B., & Wold, B. (1992) *Biochemistry 31*, 70–81.
Moser, H. E., & Dervan, P. B. (1987) *Science 238*, 645–650.
Nair, V., & Chamberlain, S. D. (1984) *Synthesis*, 401–403.
Ono, A., Ts'O, P. O. P., & Kan, L. (1991a) *J. Am. Chem. Soc. 113*, 4032–4033.
Ono, A., Chen, C.-N., & Kan, L. (1991b) *Biochemistry 30*, 9914–9921.
Pilch, D. S., Levenson, C., & Shafer, R. H. (1991) *Biochemistry 30*, 6081–6087.
Radhakrishnan, I., Gao, X., de los Santos, C., Live, D., & Patel, D. J. (1991a) *Biochemistry 30*, 9022–9030.
Radhakrishnan, I., de los Santos, C., & Patel, D. J. (1991b) *J. Mol. Biol. 221*, 1403–1418.
Rajagopal, P., & Feigon, J. (1989) *Nature 339*, 637–640.
Ratner, L., Haseltine, W., Patarca, R., Livak, K. J., Starcich, B., Josephs, S. F., Doran, E. R., Rafalski, J. A., Whitehorn, E. A., Baumeister, K., Ivanoff, L., Petteway, S. R., Jr., Pearson, M. L., Lautenberger, J. A., Papas, T. S., Ghrayeb, J., Chang, N. T., Gallo, R. C., & Wong-Staal, F. (1985) *Nature 313*, 277–284.
Sambrook, J., Fritsch, E. F., Maniatis, T. (1989) in *Molecular Cloning: A Laboratory Manual*, 2nd ed., Cold Spring Harbor Laboratory Press, Cold Spring Harbor, NY.
Sanger, F., Nicklen, S., & Coulson, A. R. (1977) *Proc. Natl. Acad. Sci. U.S.A. 72*, 2251–2255.
Singleton, S. F., & Dervan, P. B. (1992a) *J. Am. Chem. Soc. 114*, 6957–6965.
Singleton, S. F., & Dervan, P. B. (1992b) *Biochemistry 31*, 10995.
Sinha, N. D., Biernat, J., McManus, J., & Koster, H. (1984) *Nucleic Acids Res. 12*, 4539–4557.
Strobel, S. A., Doucette-Stamm, L. A., Riba, L., Housman, D. E., & Dervan, P. B. (1991) *Science 254*, 1639–1642.